The Science Driving the 12 GeV Upgrade OF CEBAF

Jefferson Lab

February 2001

Jefferson Lab is managed and operated by the Southeastern Universities Research Association (SURA) for the U.S. Department of Energy.

Thomas Jefferson National Accelerator Facility
12000 Jefferson Avenue
Newport News
Virginia 23606
www.JLab.org
(757)-269-7100

Abstract

This White Paper presents the compelling scientific case for upgrading the Continuous Electron Beam Accelerator Facility (CEBAF) at Jefferson Lab to 12 GeV. Such a facility will make profound contributions to the study of nuclear matter. In particular, it will allow breakthrough programs to be launched in two key areas:

- *The experimental observation of the QCD flux tubes which cause confinement.* Theoretical conjectures, now confirmed by lattice QCD simulations, indicate that the most spectacular new prediction of QCD – quark confinement – occurs through the formation of a string-like "flux tube" between quarks. This conclusion (and proposed mechanisms of flux tube formation) can be tested by determining the spectrum of the gluonic excitations of mesons.
- *The measurement of the quark and gluon wavefunctions of the nuclear building blocks.* A vast improvement in our knowledge of the fundamental structure of the proton and neutron can be achieved. Not only can existing "deep inelastic scattering" cross sections be extended for the first time to cover the critical region where their basic three-quark structure dominates, but also measurements of new "deep exclusive scattering" cross sections will open the door to a new, more complete characterization of these wavefunctions by providing direct access to information on the correlations among the quarks.

In addition to opening up these qualitatively new areas of research, the Upgrade will:

- *Open important new research domains in key areas already under investigation.* These new research thrusts include:
  - Determining the dynamics underlying the quark-gluon wavefunctions through measurements of the high-momentum-transfer behavior of form factors.
  - Mapping out and understanding the transition from the hadronic to the quark-gluonic description of strongly interacting matter through the study of low-energy duality.
  - Searching for the onset of color transparency effects in the region where they are supposed to exist.
  - Determining the role of color polarization effects in the NN force by measuring the threshold ψN cross section.
  - Executing a unique and global study of short-range correlations in nuclei.
  - Examining the role of quark masses in determining hadron spectra by mapping out the currently obscure $s\bar{s}$ spectrum that straddles the boundary between the rigorously understood heavy-quark systems and the poorly understood light-quark world.

While focusing on science, this White Paper also summarizes reports on the required detector and accelerator upgrades so that it can serve as an overview of the entire plan for the 12 GeV project.

2.B Campaign 2: How are the Nuclear Building Blocks Made from Quarks and Gluons?

This section describes the dramatic progress that can be achieved in our understanding of the fundamental structure of the nuclear building blocks. One glaring gap in our knowledge exists in the region of the three basic "valence" quarks that mainly contribute at large x_{Bj}. Section 2.B.1 highlights the substantial improvements that can be reached probing parton distributions at large x_{Bj} using the deep inelastic scattering process.[1] Such a process measures a diagonal matrix element (*i.e.*, initial and final state are the same) of QCD field operators. Recently, a generalization of these parton distributions encompassing the description of exclusive processes was developed. Section 2.B.2. describes the strategy needed to verify that one is in the domain where these generalized distributions can be accessed. In the most straightforward example, deeply virtual Compton scattering, one can gain supplementary information on partons in the intermediate and large x_{Bj} region. Here one accesses non-diagonal matrix elements of QCD field operators. Similarly, in this framework hadronic form factors access a non-diagonal matrix element of local QCD field operators. Thus, hadronic form factors are related to the same generalized parton distribution functions. As such, we highlight in Section 2.B.3 the substantial progress one can reach in hadronic form factor measurements.

Deep inelastic inclusive scattering shows that scaling at modest Q^2 and ν already arises from very few resonance channels. This duality reflects the transition from strongly interacting matter to a quark-gluon theory, and thus is of fundamental importance. If quantitatively understood, low-energy quark-hadron duality can be used to obtain precise constraints for parton distributions at even larger x_{Bj}. This is described in Section 2.B.4. Lastly, in semi-inclusive meson production the scattering and production mechanisms factorize at high energy. To what extent this factorization applies at lower energy is an open question. Confirmation of factorization at lower energies would open a rich semi-inclusive program, as discussed in Section 2.B.5, allowing an unprecedented spin/flavor decomposition of parton distributions.

[1] In this section x_{Bj} is used for "Bjorken-x", the deep inelastic scattering scaling variable (which ranges from $0 \to 1$) rather than the simpler notation, x, used in the executive summary. This has been done to avoid confusion with the variable x used in the Generalized Parton Distributions (GPD's) discussed in this section; for the GPD's, x denotes the generalized parton momentum distribution (which ranges from $-1 \to 1$ because it includes the antiquark distribution).

2.B.1 Valence Quark Momentum Distributions

One of the most fundamental properties of the nucleon is the structure of its valence quark distributions, since they are the irreducible kernel of each hadron. Sea quarks, which at very high Q^2 are largely generated in perturbative QCD through gluon bremsstrahlung and subsequent splitting into quark-antiquark pairs, at low Q^2 represent one source of the nonperturbative "meson cloud contributions" that act as "dressing" on the valence quarks. At higher x values these $q\bar{q}$ complications drop away, and the simple physics of the valence quark model is exposed [Is99].

Experimentally, most of the recent studies of nucleon structure have emphasized the small-x_{Bj} region populated mainly by sea quarks (x_{Bj} being the fraction of momentum of the nucleon carried by the quark), while the valence quark structure has for some time now been thought to be understood. Three decades of deep inelastic and other high-energy scattering experiments have provided a detailed map of the nucleon's quark distributions over a large range of kinematics with one major exception – the deep valence region, at very large x_{Bj} ($x_{Bj} \gtrsim 0.5$). In this region the valence structure of the nucleon can be probed most directly, since sea quark distributions, which must be subtracted from the measured cross sections to reveal the valence structure, are negligibly small beyond $x_{Bj} \sim 0.2 - 0.3$. It is both surprising and unfortunate that the large-x_{Bj} region has been so poorly explored experimentally.

This situation is clearly evident in the valence u and d quark distributions, which are usually obtained from measurements of the proton and neutron structure functions, F_2^p and F_2^n, respectively. At leading order these functions are defined as the charge-squared weighted sums of the quark and antiquark distributions of various flavors ($q = u, d, s, \ldots$):

$$F_2(x_{Bj}) \;=\; 2x_{Bj}F_1(x_{Bj}) \;=\; x_{Bj} \sum_q e_q^2 \left(q(x_{Bj}) + \bar{q}(x_{Bj})\right) \;. \tag{7}$$

While the u quark distribution is relatively well constrained by the F_2^p data for $x_{Bj} < 0.8$, the absence of free neutron targets has left large uncertainties in the d quark distribution beyond $x_{Bj} \sim 0.5$ arising from incomplete understanding of the nuclear medium modifications in the deuteron, from which F_2^n is extracted. For instance, depending on whether one does or does not correct for Fermi motion and binding (off-shell) effects in the deuteron, the extracted $R^{np} \equiv F_2^n/F_2^p$ ratio can differ by $\sim 50\%$ already at $x_{Bj} \sim 0.75$ [Me96, Wh92] (see Fig. 24).

These large uncertainties have prevented answers to such basic questions as why the d quark distribution at large x_{Bj} appears to be smaller (or "softer") than that of the u, softer even than what would be expected from flavor symmetry. Furthermore, since the precise $x_{Bj} \to 1$ behavior of the d/u ratio is a critical test of the mechanism of spin-flavor symmetry breaking, the large errors on

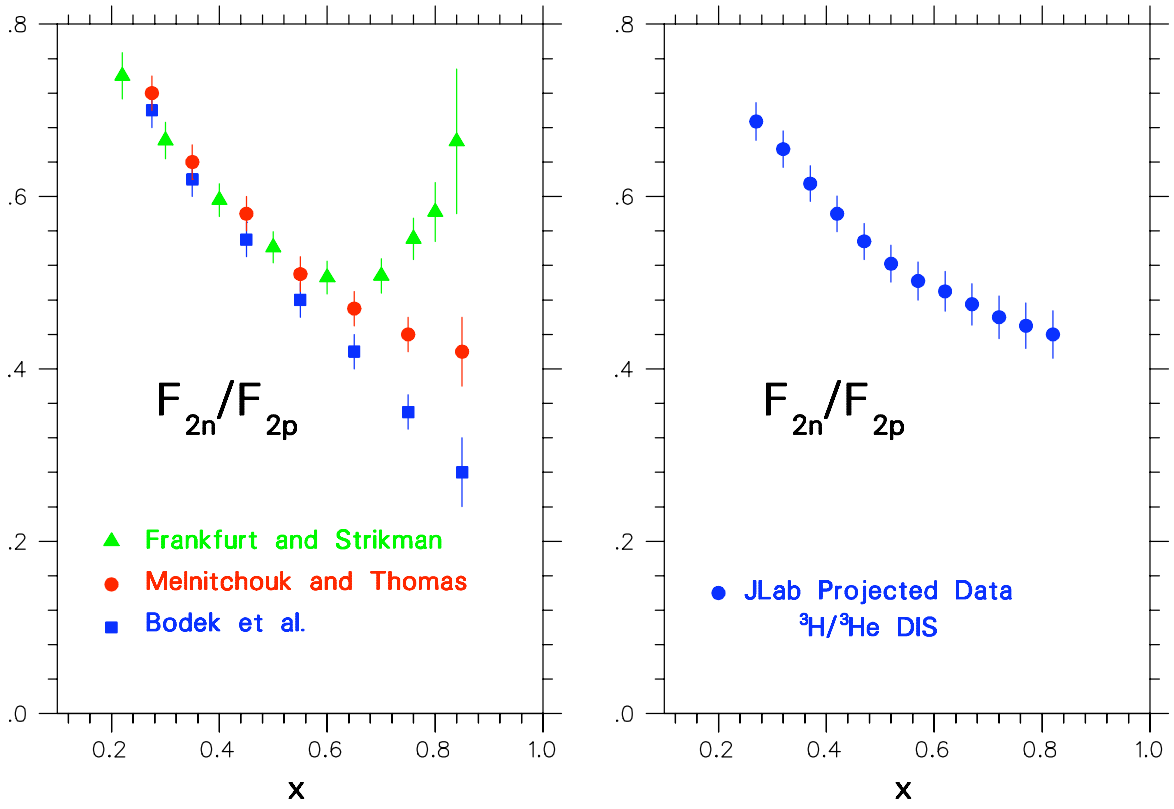

Figure 24: Ratio R^{np} of neutron to proton structure functions as a function of x_{Bj}, extracted from the SLAC data on the deep inelastic proton and deuteron structure functions. The left panel represents R^{np} extracted according to different prescriptions for treating nuclear effects in the deuteron: Fermi smearing only [Bo81, Wh92], Fermi motion and nuclear binding corrections [Me96], and assuming the nuclear EMC effect in the deuteron scales with nuclear density [Fr88]. The right panel shows the projected data with total (statistical, systematic, and model-dependent) errors for the proposed ^{3}H and ^{3}He JLab experiment.

the current data preclude any definitive conclusions about the fundamental nature of quark-gluon dynamics in the valence quark region. From another perspective, knowledge of quark distributions at large x_{Bj} is also essential for determining high-energy cross sections at collider energies, such as in searches for new physics beyond the standard model [Ku00], where structure information at $x_{Bj} \sim 0.6 - 0.8$ feeds down to lower x_{Bj} at higher values of Q^2 through perturbative Q^2 evolution.

The need for reliable large-x_{Bj} data is even more pressing for the spin-dependent quark distributions. Spin degrees of freedom allow access to information about the structure of hadrons not available through unpolarized processes. Spin-dependent quark distributions are usually extracted from measurements of the spin-polarization asymmetry, A_1, which is approximately given by the ratio of spin-dependent to spin-averaged structure functions:

$$A_1(x_{Bj}) \approx \frac{g_1(x_{Bj})}{F_1(x_{Bj})} , \tag{8}$$

where, to leading order,

$$g_1(x_{Bj}) = \sum_q e_q^2 \ (\Delta q(x_{Bj}) + \Delta\bar{q}(x_{Bj})) , \tag{9}$$

with Δq defined as the difference between quark distributions with spin aligned and anti-aligned with the spin of the nucleon, $\Delta q = q \uparrow - q \downarrow$. The first spin structure function experiments at CERN [As88] on the moment, or integral, of g_1, suggested that the total spin carried by quarks was very small, or even zero, prompting the so-called "proton spin-crisis". A decade of subsequent measurements of spin structure functions using proton, deuteron, and ^{3}He targets have determined the total quark spin much more accurately, with the current world average value being $\sim 30\%$ [La98a], which is still considerably less than the value expected from the most naïve quark model in which valence quarks carry all of the proton spin.

While the spin fractions carried by quarks and gluons (or generically, partons) are obtained by integrating the spin-dependent parton momentum distributions, the distributions themselves, as a function of the momentum fraction x_{Bj}, contain considerably more information about the quark-gluon dynamics than their integrals do. Furthermore, the spin-dependent distributions are generally even more sensitive than the spin-averaged ones to the quark-gluon dynamics responsible for spin-flavor symmetry breaking. Considerable progress has been made in measuring spin-dependent structure functions over the last decade, especially in the small x_{Bj} region. However, relatively little attention has been paid to the polarized structure functions in the pure valence region at large x_{Bj}. The lack of data in the valence region is particularly glaring in the case of the neutron, where there is no information at all on the polarization asymmetry A_1^n for $x_{Bj} \geq 0.4$. This is unfortunate, since there are rigorous QCD predictions for the behavior of A_1 as $x_{Bj} \to 1$ that have never been tested.

Theoretical predictions for large-x_{Bj} distributions

The simplest model of the proton, polarized in the $+z$ direction, has three quarks described by a wavefunction that is symmetric in spin and flavor [Cl73]:

$$\begin{aligned} |p\uparrow\rangle \;\; = \;\; & \frac{1}{\sqrt{2}}\,|u\uparrow(ud)_{S=0}\rangle \;+\; \frac{1}{\sqrt{18}}\,|u\uparrow(ud)_{S=1}\rangle \;-\; \frac{1}{3}\,|u\downarrow(ud)_{S=1}\rangle \\ & -\frac{1}{3}\,|d\uparrow(uu)_{S=1}\rangle \;-\; \frac{\sqrt{2}}{3}\,|d\downarrow(uu)_{S=1}\rangle\;, \end{aligned} \tag{10}$$

where $q\uparrow\downarrow$ represents the active quark that undergoes the deep inelastic collision, and $(qq)_S$ denotes the two-quark configuration with spin S that is a spectator to the scattering. (The neutron wavefunction can be obtained by simply interchanging the u and d quarks in this expression.) On the basis of exact spin-flavor symmetry, which is described by the group SU(6), the $S = 0$ and $S = 1$ "di-quark" states contribute equally, giving rise to simple relations among the quark distributions, such as $u = 2d$ and $\Delta u = -4\Delta d$, which in terms of the structure functions correspond to:

$$R^{np} \equiv F_2^n/F_2^p = \frac{2}{3};\quad A_1^p = 5/9;\quad \text{and}\quad A_1^n = 0. \tag{11}$$

In nature the spin-flavor SU(6) symmetry is, of course, broken. It has been known for some time that the d quark distribution is softer than the u quark distribution, reflecting the fact that the neutron-to-proton ratio R^{np} (shown in Fig. 24) deviates strongly from the SU(6) expectation beyond $x_{Bj} \sim 0.4$. On the other hand, the data for the polarization asymmetries A_1^p and A_1^n (shown in Fig. 25) are so poor in the valence region that it is presently not possible to discern whether the SU(6) predictions are borne out for the spin-dependent distributions.

A number of models have been developed for quark distributions that incorporate mechanisms for the breaking of the SU(6) symmetry; some of these models can be linked directly to phenomena such as the hyperfine splitting of the baryon and meson mass spectra. Feynman and others [Fe72, Cl73, Ca75a] observed that there was a correlation between the nucleon and Δ mass difference and the suppression of R^{np} at large x_{Bj}. A quark hyperfine interaction, such as that due to one-gluon exchange, instantons or pion exchange (which can induce a higher energy for the $S = 1$ spectator "di-quark" in Eq.(10)) will necessarily give rise to a larger mass for the Δ since the quark wavefunction for the Δ has all "di-quark" configurations with $S = 1$. If the $S = 0$ states are dominant at large x_{Bj}, Eq.(10) implies that the d quark distribution will be suppressed relative to that of the u in the valence quark region. This expectation has, in fact, been built into most phenomenological fits to the parton distribution data [Ei84, Di88, Ma94a, La95]. This mechanism also leads to specific predictions for the polarization asymmetries as $x_{Bj} \to 1$:

$$R^{np} \to \frac{1}{4};\quad A_1^p \to 1;\quad \text{and}\quad A_1^n \to 1\;. \tag{12}$$

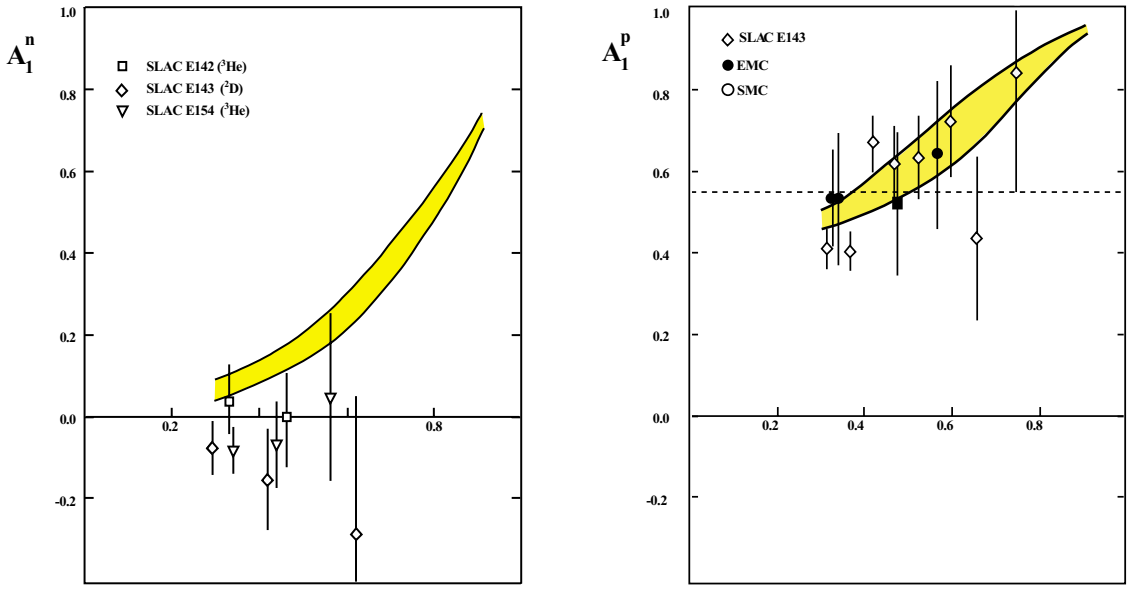

Figure 25: Sample of large-x_{Bj} data for A_1^n (left) and A_1^p (right). The predictions of SU(6) for $x_{Bj} \to 1$ are $A_1^n = 0$ and $A_1^p = 5/9$ (dashed line). The shaded bands are broken SU(6) valence quark model predictions versus x_{Bj} for A_1^n and A_1^p, as evaluated in Ref. [Is99].

More radical nonperturbative models of SU(6) breaking, such as those which include instantons as important degrees of freedom, predict dramatically different behavior for A_1^n as $x_{Bj} \to 1$; *i.e.*, that it goes to a low value close to zero [Ko97, Kopc].

Arguments based on perturbative QCD, on the other hand, predict that the dominant components of the proton valence wavefunction at large x_{Bj} are those associated with states in which the total "di-quark" spin projection, S_z, is zero [Fa75]. Consequently, scattering from a quark polarized in the opposite direction to the proton polarization is suppressed relative to the helicity-aligned configuration. From Eq.(10) this leads to the predictions in the $x_{Bj} \to 1$ limit:

$$R^{np} \to \frac{3}{7}; \quad A_1^p \to 1; \quad \text{and} \quad A_1^n \to 1 \; . \tag{13}$$

The novelty of these predictions, especially for A_1^p and A_1^n, is that they follow essentially directly from perturbative QCD in the limit of $Q^2 \to \infty$ and $x_{Bj} \to 1$. However, it is not clear *a priori* at which x_{Bj} and Q^2 the transition from the nonperturbative dynamics, embodied in the predictions (12), to perturbative QCD takes place, so experimental guidance on this issue is essential.

While the trend of the existing R^{np} data is consistent with models with broken SU(6) symmetry, they cannot discriminate between the competing mechanisms of SU(6) breaking (as evident from Fig. 24) because of uncertainties in the extraction procedure associated with nuclear corrections. For the asymmetries A_1^n and A_1^p, while we do not expect the SU(6) predictions to be accurate, the existing measurements at high x_{Bj} lack the precision to even distinguish any of the predictions from the naïve SU(6) result.

The ratio $R^{np} = F_2^n/F_2^p$ of the neutron and proton structure functions

If the nuclear EMC effect (the modification of the free nucleon structure function in the nuclear environment) in deuterium were known, one could apply nuclear smearing corrections directly to the deuterium data to obtain the free neutron F_2^n. However, the EMC effect in the deuteron requires knowledge of the free neutron structure function itself, so the argument becomes cyclic. The best way to reliably determine R^{np}, free of the large uncertainties associated with nuclear corrections at large x_{Bj}, is through simultaneous measurements of the inclusive ^{3}He and ^{3}H structure functions, maximally exploiting the mirror symmetry of $A = 3$ nuclei. Regardless of the absolute value of the nuclear EMC effect in ^{3}He or ^{3}H, the differences between the EMC effects in these nuclei will be small (on the scale of charge symmetry breaking in the nucleus).

In the absence of a Coulomb interaction, and in an isospin-symmetric world, the properties of a proton (neutron) bound in the ^{3}He nucleus would be identical to those of a neutron (proton) bound

in the ^{3}H nucleus. If, in addition, the proton and neutron distributions in ^{3}He (and in ^{3}H) were identical, the neutron structure function could be extracted with no nuclear corrections, regardless of the size of the EMC effect in ^{3}He or ^{3}H separately.

In practice, ^{3}He and ^{3}H are of course not perfect mirror nuclei – their binding energies for instance differ by some 10% – and the proton and neutron distributions are not quite identical. However, the $A = 3$ system has been studied for many years, and modern realistic $A = 3$ wavefunctions are known to rather good accuracy. Using these wavefunctions, together with a nucleon spectral function, the difference in the EMC effects for the ^{3}He and ^{3}H nuclei has been calculated [Af00b, Pa00, Ci90, Uc88] to be less than 2% for $x_{Bj} < 0.85$. More importantly, the actual model dependence of this difference is less than 1% for all x_{Bj} values accessible experimentally with an 11 GeV beam.

By performing the tritium and helium measurements under identical conditions, the ratio of the deep inelastic cross sections for the two nuclei can be measured with 1% experimental uncertainty (SLAC Experiments E139 [Go94] and E140 [Da94, Ta96] have quoted 0.5% uncertainties for measurements of ratios of cross sections). Deep inelastic scattering with the proposed 11 GeV JLab electron beam can therefore provide precise measurements for the $F_2^{^3\mathrm{He}}/F_2^{^3\mathrm{H}}$ ratio, from which R^{np} can be extracted essentially free of nuclear corrections at the 1% level over the entire range $0.10 \leq x_{Bj} \leq 0.82$. In addition, it will for the first time enable the size of the EMC effect to be determined in $A = 3$ nuclei, which to date has been measured only for $A \geq 4$ nuclei. The key issue for this experiment will be the availability of a high-density tritium target, comparable with the previously used Saclay [Am94] and MIT-Bates [Be89] tritium targets. The quality of the projected data is highlighted in Fig. 24 and in Fig. 6 of the executive summary.

The neutron spin structure function A_1^n

While data on R^{np} and A_1^p give some indication of the large-x_{Bj} behavior of the valence quark distributions at $x_{Bj} \lesssim 0.5$, the experimental situation for the neutron A_1^n at large x_{Bj} is totally unclear. The statistical precision of the data available does not even allow a meaningful statement about the qualitative behavior of A_1^n for $x_{Bj} > 0.4$. The experiment proposed here, as outlined in the executive summary, will use the 11 GeV JLab electron beam to perform a precision measurement of A_1^n, utilizing the Hall A polarized ^{3}He target and the proposed MAD (Medium-Acceptance Device) spectrometer. Because the neutron in ^{3}He carries almost 90% of the nuclear spin, polarized ^{3}He is an ideal source of polarized neutrons [Fr90].

The experiment involves measurement of the polarization asymmetry, $A_1^{^3\mathrm{He}}$, defined as:

$$A_1^{^3\mathrm{He}}(x_{Bj}) \approx \frac{1}{D}\frac{d\sigma^{\uparrow\downarrow} - d\sigma^{\uparrow\uparrow}}{d\sigma^{\uparrow\downarrow} + d\sigma^{\uparrow\uparrow}} \ , \tag{14}$$

where $d\sigma^{\uparrow\uparrow}$ ($d\sigma^{\uparrow\downarrow}$) is the cross section for scattering polarized electrons from a polarized ^{3}He target with the beam and target helicities parallel (antiparallel) and D is a kinematic factor relating the virtual photon polarization to that of the electron. The neutron asymmetry A_1^n is extracted from $A_1^{^3\mathrm{He}}$ after correcting for residual nuclear effects in ^{3}He associated with Fermi motion and binding, using modern three-body wavefunctions [Wo89, Ci93a, Sc93], similar to those used in correcting for nuclear effects in $F_2^{^3\mathrm{He}}$ discussed in the previous section. Furthermore, because the asymmetry is a ratio of nuclear structure functions, the nuclear effects on A_1^n will be considerably smaller than those associated with absolute structure functions. In addition to the use of the polarized ^{3}He target, other polarized targets (ND_3 and NH_3)will be used for cross checks and for the investigation of the nuclear effects.

An example of the kinematics relevant for this experiment is given in Table 2. (Note that substantial improvements in the measurement of A_1^p at large x_{Bj}, or A_1^n at large x_{Bj} using polarized solid-state NH_3 and ND_3 targets, would also be possible with an 11 GeV cw beam). To illustrate the improvement of the projected results obtainable with JLab at 11 GeV compared with previously measured data from other facilities we introduce a figure of merit (FOM) $= D^2 \times \mathrm{Rate} \times f^2$, which allows a meaningful comparison between different laboratories. Here "Rate" takes into account the use of the proposed Medium-Acceptance Device spectrometer, and f is the dilution factor defined as the ratio of polarized nucleons to the total number of nucleons in the target. Table 2 shows the comparison between the relevant parameters at competitive existing laboratories at comparably large x_{Bj} and Q^2. Note that with increasing beam energy the depolarization factor decreases. The lowest beam energy, therefore, which guarantees access to the large-x_{Bj} region in the Bjorken limit is optimal. The anticipated data are shown in Fig. 26. JLab at 11 GeV would enable access to $x_{Bj} \lesssim 0.8$ at $W^2 \approx 4$ GeV.

Higher-twist effects and the g_2^n structure function

While the g_1 structure function has a simple interpretation in the quark-parton model in terms of quark helicity distributions and has been the focus of extensive experimental programs over the last decade, there have been few dedicated experimental studies of the g_2 structure function. The g_2 structure function is related to the transverse polarization of the nucleon, and although it does not have a simple quark-parton model interpretation, it contains important information about quark-gluon correlations within the nucleon.

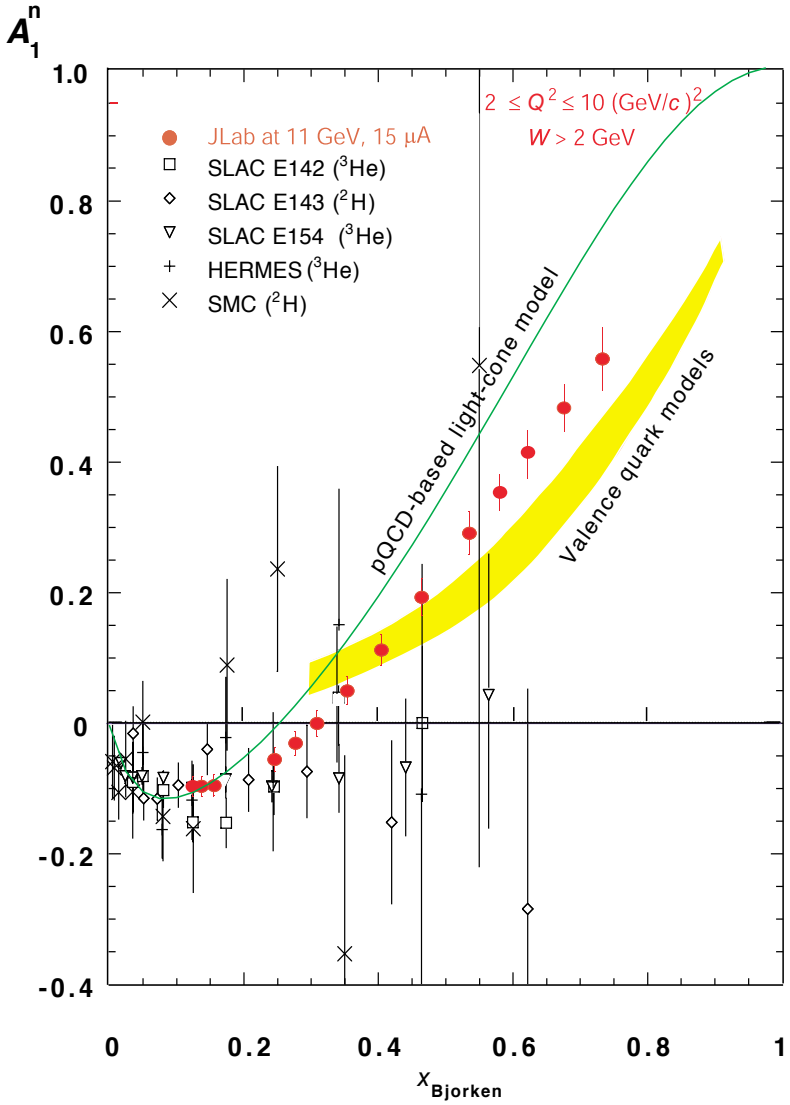

Figure 26: Simulated data for a measurement of A_1^n in the large Bjorken-x region, where it is determined by the spin structure of the valence quarks, made possible by the proposed 12 GeV Upgrade.

Table 2: Comparison of the figure of merit (FOM) for large x_{Bj} measurements of the A_1^n structure function at HERA, SLAC, and JLab.

Expt. name	E_i (GeV)	E' (GeV)	θ (deg.)	x_{Bj} bin	Q^2 $(\mathrm{GeV}/c)^2$	D	f	Rate (Hz)	FOM (10^{-4})
HERMES	35.0	17.0	5.2	0.60-0.70	9.1	0.22	0.3	0.05	2
SLAC E143	29.13	25.5	7.0	0.60-0.70	9.1	0.29	0.2	0.3	10
JLab	11.0	4.4	25	0.60-0.70	8.5	0.67	0.3	2.7	1000

In QCD the quark-gluon correlations are associated with so-called higher twist operators (where "twist" is defined as the difference between dimension and spin of an operator), which are suppressed by additional factors of $1/Q$ relative to the leading twist contribution (which is associated with free quark scattering). At large values of Q^2, QCD allows one to relate moments of spin structure functions to the matrix elements of operators of given twist. The simplest twist-3 matrix element that contains information on quark-gluon correlations is given by:

$$d_2(Q^2) \;=\; \int_0^1 dx_{Bj}\; x_{Bj}^2 \left[2g_1(x_{Bj},Q^2) + 3g_2(x_{Bj},Q^2)\right] \tag{15}$$

Note that because of the x_{Bj}^2 weighting in Eq.(15), d_2 is dominated by the large-x_{Bj} behavior of g_1 and g_2. The physical significance of d_2 is that it reflects the response of a quark to the polarization of the gluon color field in the nucleon, $d_2 = (2\chi_B + \chi_E)/3$, with χ_B (χ_E) the gluon-field polarizability in response to a color magnetic (electric) field $\vec{B}$ ($\vec{E}$) [St95].

Published data for g_2 were obtained from experiments E142-E155 at SLAC [Ab96] and the SMC experiment at CERN [Ad93]. The world's best data will soon be published from the recent E155x experiment at SLAC, which measured g_2 for proton and deuteron. Using preliminary results from this experiment [Bo00], values for g_2 for the neutron were extracted and are shown in Fig. 27. The curve labeled "g_2^{WW}" represents the leading twist contribution to g_2 [Wa77]. Using these data, a nonzero positive value for d_2^n has been extracted that is in disagreement with all of the theoretical calculations. However, in most cases, the disagreement is less than 1σ, and the size of the experimental error does not allow one to make a conclusive statement about the importance of higher-twist effects in the nucleon.

A 12 GeV JLab experiment will make a factor of 10 statistical improvement in the error on d_2^n, by taking advantage of the high-luminosity 11 GeV beam and the large-acceptance MAD spectrometer. Precision data for g_2 will be obtained in the range $0.15 \leq x_{Bj} \leq 0.8$, $W > 2$ GeV, for example at $Q^2 = 5$ $(\mathrm{GeV}/c)^2$, with special focus on the high-x_{Bj} region which dominates d_2. Projected uncertainties for such an experiment are indicated by the squares in Fig. 27.

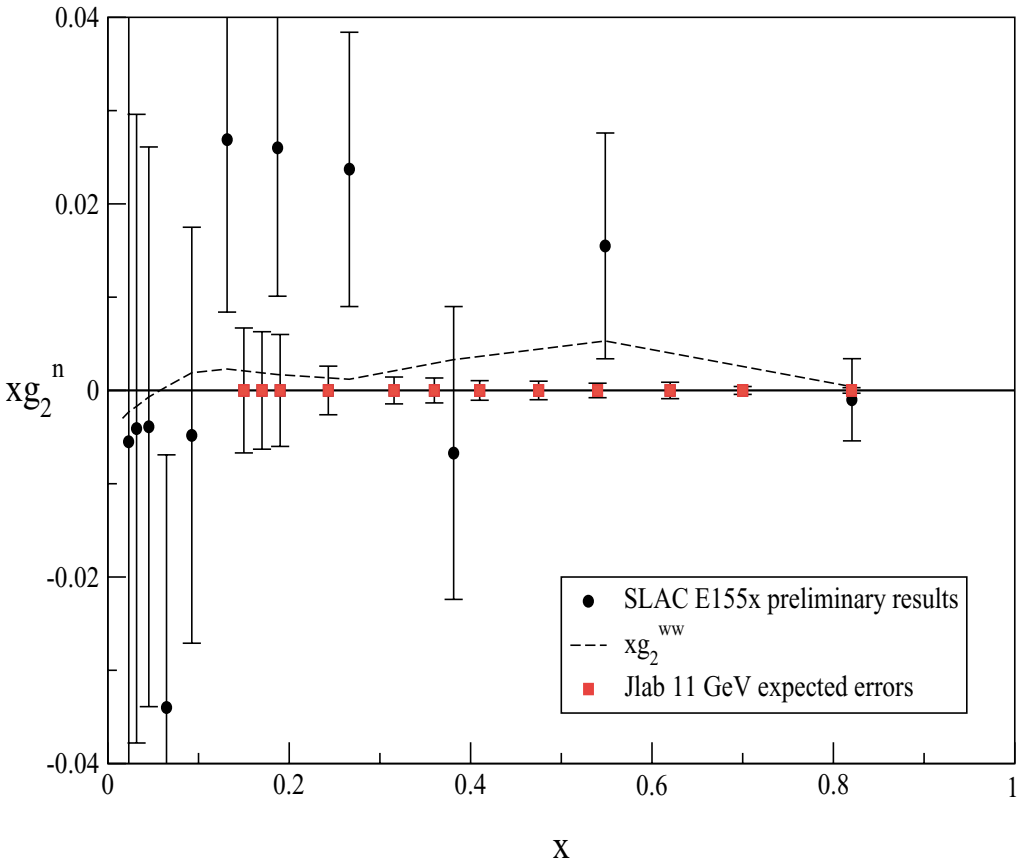

Figure 27: The preliminary results for the g_2^n spin structure function from SLAC experiment E155x. The dashed curve shows the Wandzura-Wilczek [Wa77] calculation of the leading twist contribution to g_2^n. The open squares are the expected uncertainties from an 11 GeV JLab measurement.